ISSN 1063-7826, Semiconductors, 2018, Vol. 52, No. 16, pp. 2135–2139. © Pleiades Publishing, Ltd., 2018.

26th INTERNATIONAL SYMPOSIUM “NANOSTRUCTURES: PHYSICS AND TECHNOLOGY”. NANOSTRUCTURE TECHNOLOGY

Monte Carlo Simulation of Ga Droplet Movement during the GaAs Langmuir Evaporation[1]

A. A. Spirina[a,b,*], A. G. Nastovjak[a], I. G. Neizvestny[a,b], and N. L. Shwartz[a,b]
[a] *A.V. Rzhanov Institute of Semiconductor Physics SB RAS, Novosibirsk, Russia*
[b] *Novosibirsk State Technical University, Novosibirsk, 630073 Russia*
**e-mail: spirina.anna.alex@gmail.com*

Abstract—A kinetic lattice Monte Carlo model is used to study the Ga droplets self-propelled motion along GaAs(111)A and (111)B surfaces during the initial stage of high-temperature annealing. An estimation of the droplet velocity, running along (111)A and (111)B surfaces, in a wide temperature range, is carried out. The mechanism of small Ga drops movement during high-temperature annealing is suggested. Different directions of droplets motion and the morphology of drop-crystal interface on (111)A and (111)B substrates are determined by a difference in the etching rate of (111)A and (111)B facets by liquid gallium. It is shown that metal droplets can cause step bunching.

DOI: 10.1134/S1063782618160340

1. INTRODUCTION

The interest in metal droplets motion is due to the role the droplets play in such technologies as droplet epitaxy and nanowire growth. In these techniques droplets are formed from the metal atoms deposited on the surface by an external flux. Metal droplets can be created also during the $A^{III}B^{V}$ semiconductor Langmuir evaporation [1–4]. Most of the experiments on Langmuir evaporation were carried out on GaAs(100) substrates [1, 3, 5–8]. Experimentally, it was demonstrated that group III droplets spontaneously move in the lateral direction during high-temperature annealing [1, 2, 5, 6]. There are only few publications devoted to running droplets on GaAs (111)A and (111)B surfaces [9]. An analysis of substrates orientation influence on the gallium droplet motion during Langmuir evaporation was carried out in [9]. Regardless of the substrate orientation, gallium droplets move along the ⟨110⟩ directions. During a prolonged annealing of the GaAs(111)A surface, the droplet motion was accompanied by the formation of two groups of pyramidal vacancy islands with different depths. Deep vacancy islands were associated with buried dislocations, flat islands—with thermal etching. At the bottom of the island with a flat base, a gallium drop was formed, which, during the annealing process, increased in size and split into daughter droplets. A large number of gallium droplets, uniformly distributed over the surface, were observed on the GaAs(111)B surface. These droplets, when moving, left a smoother trace. During the GaAs(100) substrates annealing an even smoother footprints of self-running droplets were observed, and the gallium droplet motion velocity was lower than that on the GaAs(111)B surface. The temperature dependence of droplet velocity was presented in [1]. In this work, minimal velocity corresponds to the congruent evaporation temperature. If the annealing temperature deviates from this value toward higher and lower temperatures, the droplets velocity increases. In other experimental studies [2, 7], in contrast to the results of [1], the droplet motion in the low-temperature annealing regime was not observed. At annealing temperatures below the maximal congruent evaporation temperature, the droplets did not move, decreased in size and completely disappeared in time. With the increasing temperature, the metallic droplets velocity increased. Two alternative droplet self-propelled motion mechanisms were suggested in [1, 2]. In both mechanisms the reason of droplets moving is the tendency to minimize the surface free energy. In [1] the driving motion force is the difference in the surface free energies for surfaces with different chemical potentials and in [2]—surface roughness minimization. Only big-sized running drops were considered in the experiments. In the present work we analyze a small Ga droplets motion along (111)A and (111)B surfaces during the GaAs evaporation by Monte Carlo simulation.

2. SIMULATION RESULTS

The simulation of GaAs substrates annealing was carried out for two surface orientations (111)A and (111)B in the temperature range of 800–1200 K. The

---

[1] The article is published in the original.

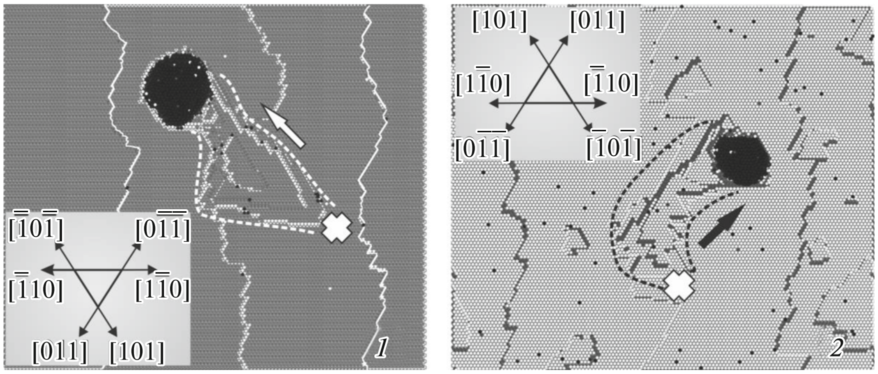

Fig. 1. Droplet movement along (111)A (*1*) and (111)B (*2*) surfaces during high-temperature annealing. Liquid Ga(*l*) is marked in black color. The arrows indicate the droplet movement directions, the cross—the droplet nucleation position; surface size 60 × 60 nm.

simulation was fulfilled, using the software developed in [10] on the base of the kinetic lattice MC model. Previously, this model was used to study the GaAs nanostructures formation by droplet epitaxy [11]. At temperatures higher than the congruent evaporation temperature T_c, the arsenic evaporation rate exceeds the gallium evaporation rate and excess gallium forms liquid droplets. Gallium evaporates in the atomic Ga form and arsenic—in the molecular As_2 form. Arsenic molecules are created on the surface during annealing by the reversible reaction $As + As \leftrightarrow As_2$ included in the model. The congruent evaporation temperature was determined for ideal (111)A and (111)B crystal surfaces: T_c (111)A = 1000 K, T_c (111)B = 900 K. Ga droplets on the (111)A surface are nucleated predominately at vicinal surface steps and, on (111)B, the droplets are formed randomly on the terraces. On the (111)B surface, even at $T < T_c$, the vacancy islands are created on the terraces during a layer-by-layer evaporation. These vacancy island edges become the source of gallium atoms for the Ga droplets nucleation at $T > T_c$. The Ga drop concentration on the GaAs(111)B surface is higher than that on the (111)A surface. The distance between the Ga droplets on the (111)A surface is determined essentially by a gallium diffusion length before evaporation and, on the (111)B surface, the arsenic evaporation plays the main role. Arsenic is more volatile than gallium. So, the arsenic diffusion length before evaporation is lower than that of gallium. Unlike the experiment, in the simulation, we can trace the motion of very small droplets.

Simulations were carried out on the vicinal surfaces with terrace width L = 20–360 nm. At temperatures $T > T_c$, the motion of gallium droplets with a diameter up to 50 nm was observed. When the droplets form on the substrate surface, the bottom and lateral liquid-crystal interfaces are formed. The lateral interface is created by the GaAs substrate etching in the vertical direction by liquid gallium and consists of six alternating facets with $\langle 111 \rangle$ orientations (three (111)A and three (111)B facets). For both surface orientations the drops move along $\langle 101 \rangle$ directions (Fig. 1). There are six equivalent directions on each surface for a droplet movement. These directions are rotated relative to each other by 60 degrees. The reason of drops motion is the GaAs etching by liquid gallium. The preferable movement direction is determined by the maximal etching rate of crystal facets. In the GaAs crystal the etching rate of the (111)A facet by liquid Ga is higher than that of the (111)B facet [12]. So, drops move toward the (111)A facet. This result is in agreement with the experimental data of Ga droplets motion on the (111) surface [2, 9].

The temperature dependences of droplets motion velocity for two substrate orientations are presented in Fig. 2. These plots correspond to the vicinal surfaces with terrace width L = 20 nm. As it is predicted in [1], the congruent evaporation temperature decreases with the L decrease (larger miscut). For L = 20 nm, T_c(111)A = 920 K and T_c(111)B = 840 K. At $T > T_c$, droplets are nucleated and start to move. At first, the drop velocity increases with the temperature rise. In the temperature range $T_c - T_c + 30$ K, the droplets on the (111)A surface move faster than on the (111)B surface. We can suggest the following explanation: on both surfaces, the drops are moving in the $\langle 101 \rangle$ direction, etching the substrate and creating lateral {111} facets. Since the (111)B facets are more stable to etching, the drop-liquid interface consists of flat (111)B facets, while (111)A facets destroy and contain kinks and their surfaces are rough. The lateral (111)A facet on the GaAs(111)B substrate is smoother than on the (111)A substrate (Fig. 2). This fact can be explained by a higher arsenic concentration on the (111)B surface near the (111)A facet, created by liquid gallium etching, and, so, by the possibility of As incorporation in kinks resulting in the (111)A facet smoothing. The rough surface etching rate is higher. That is why the etching rate of smoother (111)A facets on (111)B substrates is lower and the drop moves slower. At higher temperatures the directed motion velocity of the drop-

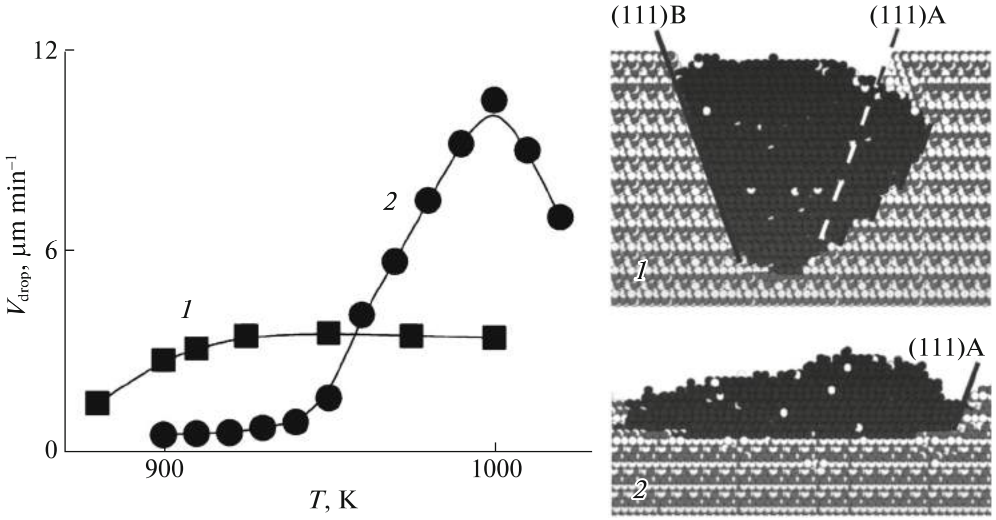

Fig. 2. (left)Temperature dependence of Ga droplet velocity: (*1*) (111)A surface, (*2*) (111)B surface; (right) cross-sections of the model substrate after the annealing at $T = 950$ K for surface orientations (111)A (*1*) and (111)B (*2*).

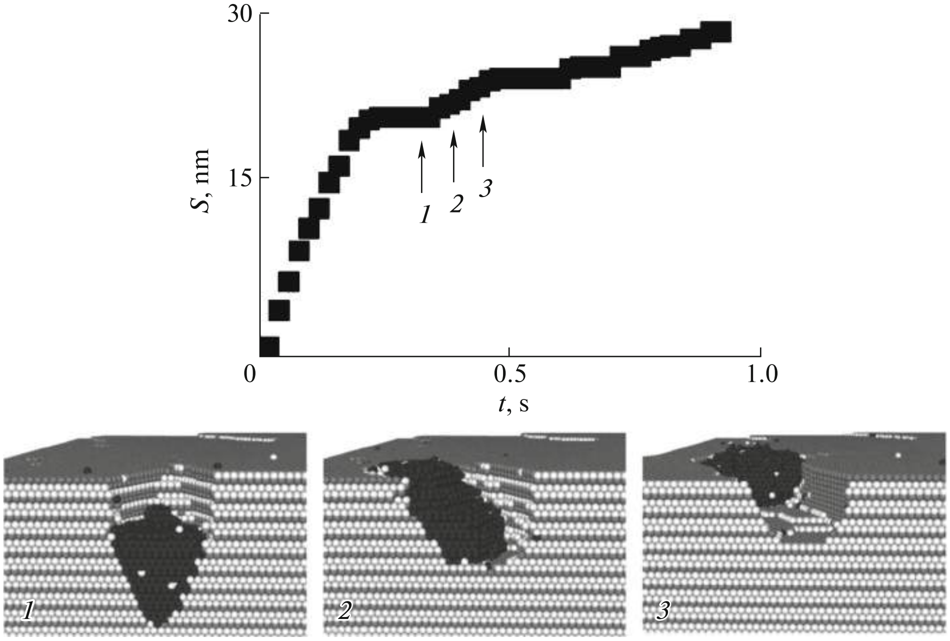

Fig. 3. Droplet distance S *versus* annealing time on GaAs(111)A surface, $T = 950$ K; cross-sections of 3D GaAs(111)A substrate after the annealing at $T = 950$ K during: (*1*) 0.35, (*2*) 0.4, (*3*) 0.45 s.

let along the (111)A surface becomes lower than that along the (111)B surface. When moving along the (111)A surface, the drop often changes its direction, leaving a trace in the triangular-shaped pits. Such a trace is observed in the experiment [9]. The dependence of the distance traveled by the droplet during the GaAs(111)A substrate annealing on time is shown in Fig. 3. At some point in time, the distance ceases to depend on time, i.e., the drop Ga stops moving. At temperatures 950–1000 K, the $S(t)$ dependence is step-like form. This is due to the drop penetration during the substrate etching by liquid gallium. Subsequently, after stopping the drop, the increase in $S(t)$ occurs due to the lateral displacement of the dipped drop. The droplet deepening and moving occurs more rapidly with the annealing temperature rise due to an increase in the substrate etching rate by liquid gallium. The GaAs(111)A substrate cross sections after the annealing at 950 K are shown in Fig. 3. With a further increase in the annealing temperatures, the gallium

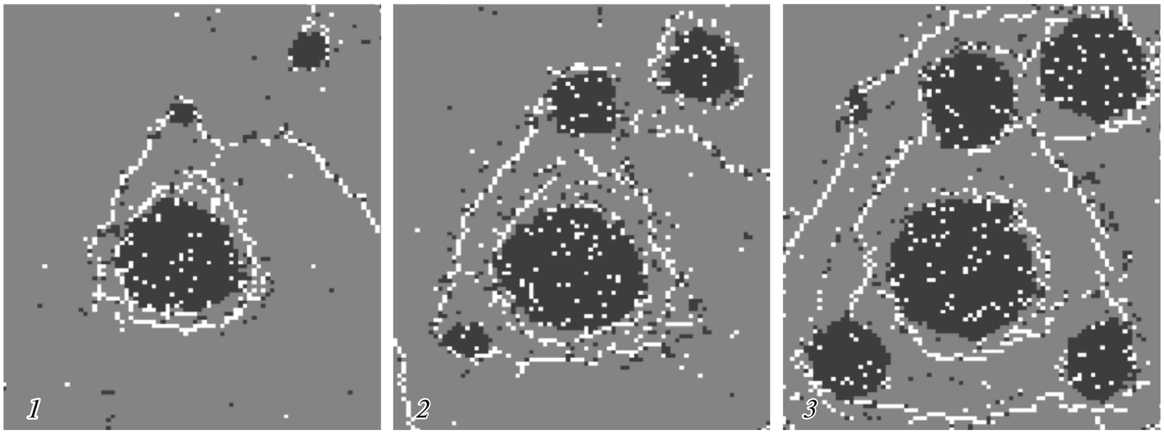

Fig. 4. Fragment 40 × 50 nm of the GaAs(111)A surface (top view) after the annealing at $T = 1060$ K during: (*1*) 0.13, (*2*) 0.135, (*3*) 0.14 s.

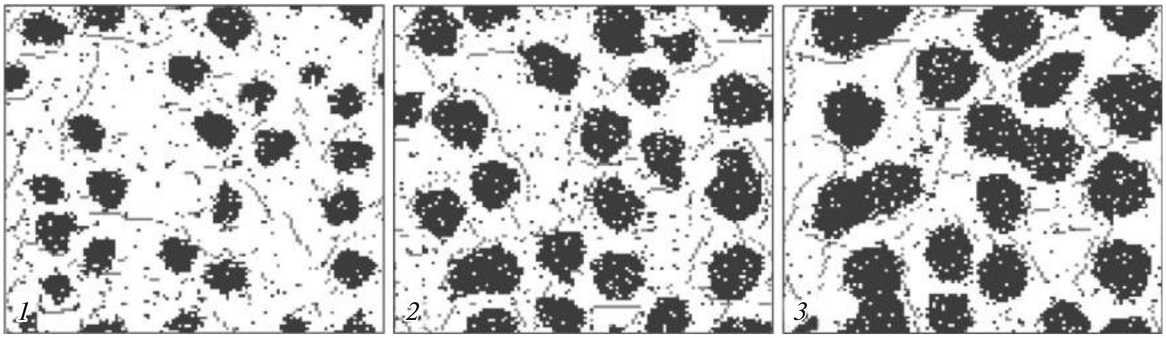

Fig. 5. Top views of the GaAs(111)B surface 60 × 60 nm after the annealing at $T = 1060$ K during: (*1*) 0.001, (*2*) 0.0025, (*3*) 0.004 s.

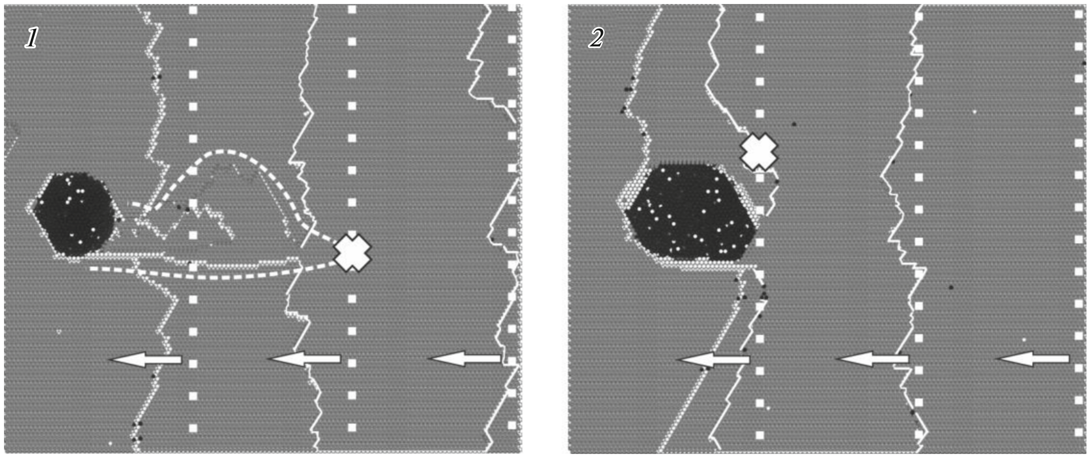

Fig. 6. Droplet and steps motion during the (111)A surface annealing at $T = 960$ K (*1*) and $T = 1020$ K (*2*). The dotted lines indicate the initial steps position, crosses—the Ga droplet nucleation position; $L = 20$ nm.

droplets after their nucleation do not practically move over the GaAs(111)A surface. The diameter of such droplets increases due to the substrate etching in the vertical and lateral directions, and that initiates the growth of triangular vacancy islands. In the corners of these islands, the "daughter" drops, the sources of which are primarily "mother" drops, are formed. The fragments of the model GaAs(111)A surface at $T = 1060$ K at different annealing times are shown in Fig. 4. On the (111)B surface, the velocity reaches its maximum at a certain temperature and a following temperature increase results in a droplet motion slowdown. An indistinct maximum is observed on the (111)A surface instead of a sharp one. The reasons for the drop deceleration at high temperatures on the (111)A and (111)B substrates are different. For the (111)A surface orientation, it is the Ga droplet embedding due to a high substrate etching rate in the vertical direction, and for the (111)B surface—a too high droplets concentration leading to drops merging (Fig. 5).

A considerable (111)A substrate etching in the vertical direction at high temperatures leads to the vicinal step movement deceleration near the Ga droplet. The images of the (111)A surface with three steps after the annealing at $T = 960$ K and $T = 1020$ K are shown in Fig. 6. At a lower temperature the substrate etching in the vertical direction is insignificant and the droplet velocity in the lateral direction is higher than that of the step velocity. The droplet trail is clearly visible in Fig. 6, *1*. At a high temperature the drop velocity in the lateral direction decreases due to the droplet displacement in the vertical direction. The droplet retards the movement of the adjacent part of the step, while the part of the step distant from the drop continues to move at the previous speed (Fig. 6, *2*).

3. CONCLUSIONS

Using the Monte Carlo simulation, the characteristics of the running Ga droplets formed on the GaAs (111)A and (111)B surfaces during the GaAs substrates Langmuir evaporation are analyzed. The mechanism of small droplets movement at the initial annealing stage is suggested. The drops start to move along ⟨101⟩ surface directions due to the GaAs etching by liquid gallium. The movement direction is determined by the difference in the etching rates of (111)A and (111)B crystal facets. The GaAs(111)A facets are etched more intensively than the (111)B facets. The droplet velocity temperature dependence has its maximum for both surface orientations. The reason for the velocity decrease at high temperatures on the (111)A surface is the drop penetration into the GaAs substrate, and on the (111)B surface—the merging of neighboring drops.

ACKNOWLEDGMENTS

The work is supported by the Russian Foundation for Basic Research (grant no. 18-02-00764) and the RAS Program.

REFERENCES

1. J. Tersoff, D. E. Jesson, and W. X. Tang, Science (Washington, DC, U. S.) **324** (5924), 236 (2009).
2. E. Hilner, A. A. Zakharov, K. Schulte, P. Kratzer, J. N. Andersen, E. Lundgren, and A. Mikkelsen, Nano Lett. **9**, 2710 (2009).
3. J. Tersoff, D. E. Jesson, and W. X. Tang, Phys. Rev. Lett. **105**, 35702 (2010).
4. C. Y. Lou and G. A. Somorjai, J. Chem. Phys. **55**, 4554 (1971).
5. J. Wu, Z. M. Wang, A. Z. Li, M. Benamara, S. Li, and G. J. Salamo, PLoS One **6** (6), 1 (2011).
6. J. Wu, Z. M. Wang, A. Z. Li, M. Benamara, and G. J. Salamo, Appl. Mater. Interfaces **3**, 1817 (2011).
7. J. Wu, Z. M. Wang, A. Z. Li, M. Benamara, J. Lee, S. D. Koukourinkova, and G. J. Salamo, J. Appl. Phys. **112**, 043523 (2012).
8. C. X. Zheng, W. X. Tang, and D. E. Jesson, Appl. Phys. Lett. **100**, 071903 (2012).
9. S. Kanjanachuchai and C. Euaruksakul, ACS Appl. Mater. Interfaces **5**, 7709 (2013).
10. A. Zverev, C. Zinchenko, N. Shwartz, and Z. Yanovitskaja, Nanotechnol. Russ. **4**, 215 (2009).
11. A. G. Nastovjak, I. G. Neizvestny, M. A. Vasilenko, and N. L. Shwartz, Semiconductors **52**, 639 (2018).
12. A. A. Spirina, A. G. Nastovjak, and N. L. Shwartz, in *Proceedings of 19th IEEE International Conference on Micro/Nanotechnologies and Electron Devices, 2018* (IEEE, Novosibirsk, 2018), p. 35.